

# Comparing lattice Dirac operators in smooth instanton backgrounds

**Christof Gattringer**<sup>a),†</sup>, **Meinulf Göckeler**<sup>a)</sup>, **C.B. Lang**<sup>b)</sup>,  
**P.E.L. Rakow**<sup>a)</sup> and **Andreas Schäfer**<sup>a)</sup>

<sup>a)</sup> Institut für Theoretische Physik  
Universität Regensburg  
93040 Regensburg, Germany

<sup>b)</sup> Institut für Theoretische Physik  
Karl-Franzens-Universität Graz  
8010 Graz, Austria

## Abstract

We compare the behavior of different lattice Dirac operators in gauge backgrounds which are lattice discretizations of a classical instanton. In particular we analyze the standard Wilson operator, a chirally improved Dirac operator and the overlap operators constructed from these two operators. We discuss the flow of real eigenvalues as a function of the instanton size. An analysis of the eigenvectors shows that overlap fermions with the Wilson operator as input operator have difficulties with reproducing the continuum zero mode already for moderately small instantons. This problem is greatly reduced when using the chirally improved operator for the overlap projection.

PACS: 11.15.Ha

Key words: Lattice QCD, instantons, Ginsparg-Wilson fermions

---

<sup>†</sup> Supported by the Austrian Academy of Sciences (APART 654).

**Introductory remarks:** Recently it was realized that the Ginsparg-Wilson equation [1] is crucial for implementing chiral symmetry on the lattice. Currently three types of exact solutions are known: The overlap operator [2], perfect actions [3] and domain wall fermions [4]. Furthermore a systematic expansion of a solution of the Ginsparg-Wilson equation was developed and tested in [5, 6]. These new lattice Dirac operators based on the Ginsparg-Wilson equation were recently used to analyze relevant excitations of the QCD vacuum which affect the Dirac operator [7, 8, 9, 10], in particular the local chirality variable proposed in [11] was studied in detail.

These studies of the excitations affecting the lattice Dirac operator are motivated by the instanton picture of chiral symmetry breaking (see [12] for extended reviews). A single instanton or anti-instanton produces a zero eigenvalue of the Dirac operator. An interacting pair of an instanton and an anti-instanton leads to a complex conjugate pair of small eigenvalues instead of two zero eigenvalues. In instanton models the QCD vacuum is pictured as a fluid of interacting instantons and anti-instantons which lead to an accumulation of small eigenvalues near the origin. Since the density of eigenvalues at the origin is related to the chiral condensate through the Banks-Casher relation [13] the fluid of instantons and anti-instantons leads to a breaking of chiral symmetry. The lattice studies [7]-[10],[14] tried to prove or refute this picture of interacting instantons and anti-instantons. To be more specific, various observables built from the eigenvectors of the Dirac operator were studied for background gauge fields generated by simulations in the quenched approximation.

A good method for testing properties of different lattice Dirac operators is to study them in smooth instanton backgrounds. In this letter we report on such a study comparing the overlap Dirac operator based on the Wilson operator [2], the standard Wilson operator, a recently proposed approximate solution of the Ginsparg-Wilson equation [5, 6] which we will refer to as the *chirally improved Dirac operator* and the overlap operator with the chirally improved operator as input operator. We analyze different properties of the eigenvectors and eigenvalues for these Dirac operators using a lattice discretization of instantons. Another study including smooth instanton backgrounds was reported in [15], which investigated the number of zero modes and the topological charge as a function of instanton radius.

The goal of our analysis is twofold: Firstly it serves to better understand the results of the above mentioned studies of relevant excitations in the QCD vacuum as seen by the lattice Dirac operator. When the instanton is large compared with the lattice spacing, all operators give good results. But when we consider smaller instanton radii we find that the overlap operator with

Wilson input operator has difficulties with reproducing the continuum zero mode in an instanton background even for moderately small instantons. We show that this problem is greatly reduced when using the chirally improved operator for the overlap projection.

The second goal of this study is to achieve a better understanding of technical aspects of the overlap projection. The sensitivity to defects should be understood, in particular if one uses an approximate solution of the Ginsparg-Wilson equation as a starting point for the overlap projection as proposed in [16].

**Technicalities:** We analyze the overlap Dirac operator, the standard Wilson Dirac operator and the chirally improved Dirac operator. The latter has been described in detail in [5]. Here, since the discretized instanton configurations are smooth, we use the coefficients for the free case as listed in the appendix of [6].

The overlap operator is given by

$$D_{ov} = 1 - \frac{1 - D_0}{\sqrt{(1 - D_0^\dagger)(1 - D_0)}}, \quad (1)$$

where  $D_0$  is any reasonable lattice version of the Dirac operator. Here we use for  $D_0$  both the standard Wilson Dirac operator leading to the *Wilson overlap operator* as well as the chirally improved operator leading to the *chirally improved overlap operator*. We construct the inverse square root using Chebychev approximation following the approach discussed in [17, 18].

A method for putting an instanton on the lattice has been proposed in Ref. [19]. Here we use a slightly modified version of this procedure. In the regular gauge, the continuum instanton potential is written as

$$A_\mu(x) = \frac{i}{2(x^2 + \rho^2)} (s_\mu \bar{s}_\nu - s_\nu \bar{s}_\mu) x_\nu, \quad (2)$$

and in the singular gauge we have

$$\tilde{A}_\mu(x) = \frac{i\rho^2}{2x^2(x^2 + \rho^2)} (\bar{s}_\mu s_\nu - \bar{s}_\nu s_\mu) x_\nu, \quad (3)$$

where  $s_4 = \bar{s}_4 = 1$ ,  $s_j = -\bar{s}_j = i\sigma_j$  ( $j = 1, 2, 3$ ) and  $\rho$  is the “radius” of the instanton. The corresponding expressions for an anti-instanton are obtained by exchanging  $s_\lambda$  and  $\bar{s}_\lambda$ .

The first step of our procedure is a coordinate transformation  $x_\mu \rightarrow y_\mu$  which maps the real line onto the interval  $(0, L)$ , where  $L$  is identified

with the length of our lattice (measured in units of the lattice spacing and assumed to be even). For this transformation we take  $x_\mu = f(y_\mu)$  with

$$f(y) = L^2 \left[ (L - y)^{-1} - y^{-1} \right]. \quad (4)$$

Acting with this transformation on the (anti-)instanton potential either in the regular or in the singular gauge we obtain the corresponding potentials on the four-torus  $(0, L)^4$ . The center of the instanton,  $x_1 = \dots = x_4 = 0$ , is mapped onto  $y_1 = \dots = y_4 = L/2$ . Note that the instanton is “squeezed” by this procedure so that the radius  $R$  of the potential on the four-torus is related to the radius  $\rho$  of its infinite-volume precursor by  $\rho = f(R + L/2)$ .

In the second step we divide our lattice into an “inner part” around  $y_1 = \dots = y_4 = L/2$  and a complementary “outer part”. According to the procedure of Ref. [19] we work with the potential in the regular (singular) gauge in the inner (outer) part using the gauge transformation connecting the two gauges to glue both potentials together. The third step consists in computing the gauge links from the potential. This is easily done analytically.

The resulting SU(2) link variables are finally embedded in SU(3) in the most trivial way, namely as  $2 \times 2$  blocks in the upper left-hand corner of the SU(3) matrices.

We work on lattices with size  $16^4$  and  $12^4$ . For the fermions we use periodic boundary conditions in space direction and anti-periodic boundary conditions in time direction. The numerical computations of eigenvalues and eigenvectors are done with the implicitly restarted Arnoldi method [20].

**The flow of real eigenvalues:** It is known that in an instanton background an exact solution of the Ginsparg-Wilson equation has exact zero eigenvalues [3], as does the continuum Dirac operator. Currently only the overlap operator shows this property. A practical implementation of perfect actions requires a finite parametrization of the lattice Dirac operator and the coefficients of the parametrization are determined from renormalization group transformations. Since an exact solution of the Ginsparg-Wilson equation is necessarily non-ultralocal [21], any practical implementation of the perfect action will be an ultralocal approximation of a solution of the Ginsparg-Wilson equation. Thus the fixed point operator as well as the chirally improved operator will only have approximate zero modes. Both these Dirac operators obey  $\gamma_5$ -hermiticity, i.e.  $\gamma_5 D \gamma_5 = D^\dagger$ . This implies [22] that eigenvectors  $\psi$  of  $D$  with eigenvalues  $\lambda$  have  $\psi^\dagger \gamma_5 \psi = 0$  unless  $\lambda$  is real. This has to be compared with the property that  $\psi^\dagger \gamma_5 \psi = 0$  unless  $\lambda$  is zero, which

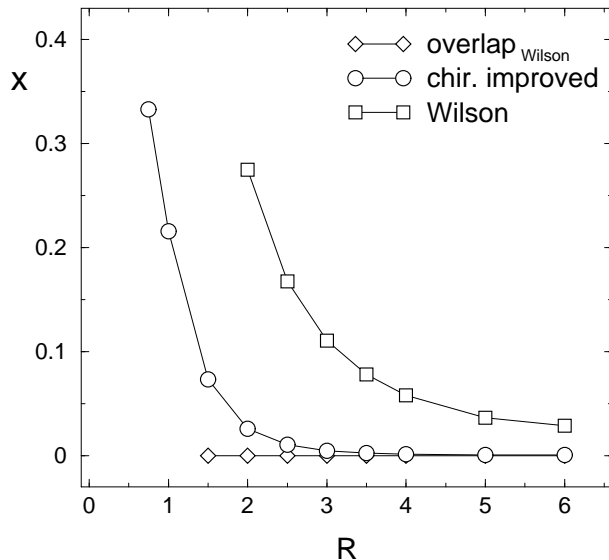


Figure 1: The dependence of the position  $x$  of the real eigenvalue (zero mode) on the radius  $R$  (in lattice units) of the underlying instanton. We show our results for the Wilson overlap operator (diamonds), the chirally improved operator (circles) and the Wilson operator (squares). The data were computed on  $16^4$  lattices.

holds for eigenvectors of an exact solution of the Ginsparg-Wilson equation or for the eigenmodes of the continuum Dirac operator. It thus follows that for perfect actions, for the chirally improved Dirac operator and also for Wilson fermions only eigenvectors with real eigenvalues are possible candidates for topological modes.

An interesting question is, how well different operators manage to project the real mode into the origin when the underlying gauge field changes. In Fig. 1 we show the position  $x$  of the real eigenvalue as a function of the radius  $R$  (in lattice units) of the underlying instanton configuration. This study was done on lattices of size  $16^4$ . We display data for the Wilson overlap operator, the chirally improved operator and the standard Wilson operator for identical gauge configurations. The behavior of the zero modes of the Wilson overlap operator is of course trivial and it serves only as a reference line. For the Wilson operator we find a very strong dependence of the real mode on the radius of the instanton. Already for large instantons

the corresponding eigenvalue is shifted to relatively large real values and this shift increases as the radius of the instanton shrinks further. The chirally improved Dirac operator is considerably less sensitive to the radius of the instanton. It starts to deviate from 0 only for radii below 2.5 lattice units.

Our analysis sheds light on a potential problem of the overlap projection: Whenever the background configurations contain defects, i.e. gauge configurations with very small excitations carrying topological charge, the overlap projection becomes numerically expensive and low eigenvalues of  $(1 - D_0^\dagger)(1 - D_0)$  have to be projected out before the square root in (1) can be evaluated numerically. The underlying mechanism is nicely illustrated in our Fig. 1: For small instanton radius the real eigenvalue of the Wilson operator  $D_0$  used in the overlap projection (1) comes close to the center of the projection (1 in the complex plane) causing the inverse square root to blow up which spoils the numerical evaluation of the overlap operator. Comparing the Wilson curve with the curve for the chirally improved operator shows that when using already an approximate solution of the Ginsparg-Wilson equation as  $D_0$  in the overlap projection [16] the problem with defects is milder.

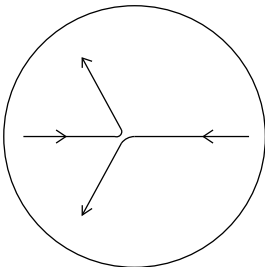


Figure 2: Schematic picture for the movement of the physical real mode and its doubler partner as a single instanton is destroyed. The circle represents the Ginsparg-Wilson circle in the complex  $\lambda$  plane, and the two other curves are the schematic trajectories of the two eigenvalues.

Fig. 1 also illustrates how topological modes are treated by solutions and approximate solutions of the Ginsparg-Wilson equation. For an exact solution of the Ginsparg-Wilson equation it is known that the spectrum depends discontinuously on the underlying gauge field. Since (1) the total number of eigenvalues is even, (2) all eigenvalues have to lie on the Ginsparg-Wilson circle (the circle with radius 1 and center 1 in the complex plane)

and (3) all modes which are not real come in complex conjugate pairs, a single eigenvalue 0 has to vanish discontinuously as the underlying gauge field is deformed from topological sector 1 to sector 0. Since an ultralocal approximation of a solution of the Ginsparg-Wilson equation cannot show such discontinuous behavior the change of the topological sector of the underlying gauge field has to manifest itself differently: As the instanton shrinks, the real mode starts to travel into the interior of the Ginsparg-Wilson circle (for an approximate solution of the Ginsparg-Wilson equation the eigenvalues are not confined to the circle) where it meets a partner from the doubler branch of the spectrum. When they meet on the real axis they can continuously form a complex conjugate pair and travel back to the outside of the circle. A schematic picture of this behavior is given in Fig. 2.

The better a Dirac operator approximates a Ginsparg-Wilson fermion, the faster the eigenvalue moves through the center of the circle. We remark that we have also seen the behavior of Fig. 2, in which a partner from the doubler sector meets the displaced real mode to form a complex conjugate pair, in a numerical study of random matrices with the same symmetries as the lattice Dirac operator.

**Localization properties of the eigenvectors:** In order to further analyze the behavior of different lattice Dirac operators in instanton backgrounds we now study properties of their eigenvectors. In the background of an instanton field the continuum Dirac operator has a zero mode  $\psi_0$  (see e.g. [12]). It is localized at the same position as the underlying instanton. A gauge invariant density  $p(x)$  which inherits this localization is obtained by summing over the color and Dirac indices  $c$  and  $\alpha$ ,

$$p(x) = \sum_{\alpha,c} \psi_0(x)_{\alpha,c}^* \psi_0(x)_{\alpha,c} = \frac{2R^2}{\pi^2(R^2 + x^2)^3}. \quad (5)$$

Due to the normalization of the zero modes we have  $\int d^4x p(x) = 1$ . A measure of the localization of  $\psi$  is given by the inverse participation ratio,

$$I = \int d^4x p(x)^2 = (5\pi^2 R^4)^{-1}. \quad (6)$$

As an alternative measure of locality [15] studies the self-correlation of the local chiral density. For different radii of our lattice instantons we computed the inverse participation ratio of the corresponding zero mode. In the plot on the left-hand side of Fig. 3 we show our results for lattice size  $16^4$ . We

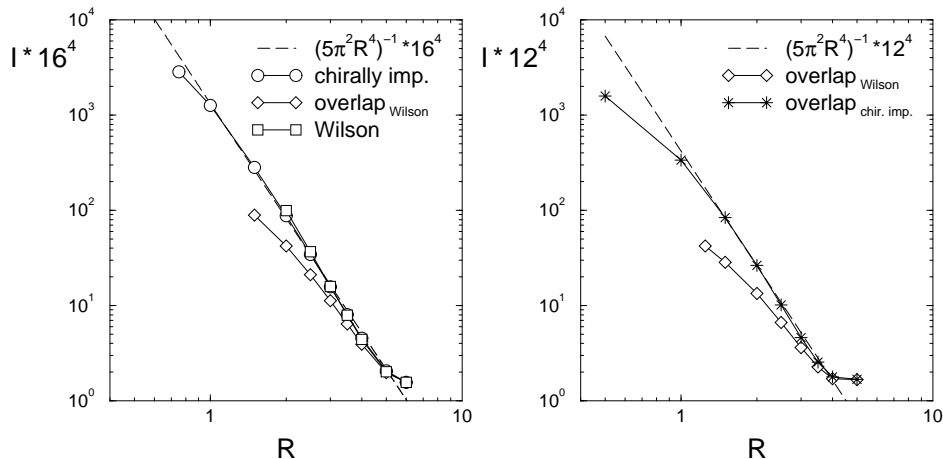


Figure 3: The inverse participation ratio of the zero mode as a function of the radius  $R$  of the underlying instanton. On the left-hand side we show our results on  $16^4$  lattices for the Wilson overlap operator (diamonds), the chirally improved operator (circles) and the Wilson operator (squares). The right-hand side plot shows a comparison of the Wilson overlap operator (diamonds) and the chirally improved overlap operator (asterisks) on  $12^4$  lattices. The dashed lines represent the continuum formula. We rescale  $I$  by the volume, i.e. we plot  $I \times 16^4$ , respectively  $I \times 12^4$ .

normalized the inverse participation ratio  $I$  by the volume<sup>1</sup>, i.e. we plot  $I \times 16^4$ . The symbols give the numerical results while the dashed line represents the continuum formula from Eq. (6). From the plot is obvious that for our largest value of the instanton radius,  $R = 6$ , the lattice results are slightly above the continuum value due to finite size effects. For smaller  $R$ , the numerical results for the two ultralocal lattice Dirac operators, i.e. the Wilson Dirac operator (squares) and the chirally improved Dirac operator (circles) follow the continuum curve down to relatively small values of  $R$ . For the chirally improved operator the agreement with the continuum result holds down to  $R = 1$  and only for  $R = 0.75$ , as the instanton begins to “fall through the lattice” we find a considerable deviation. For the Wilson operator, due to the move of the real mode into the interior of the eigenvalue distribution we could not obtain data for  $R < 2$ . However, down to  $R = 2$

<sup>1</sup>With this normalization the inverse participation ratio is a quantity widely used in solid state physics.



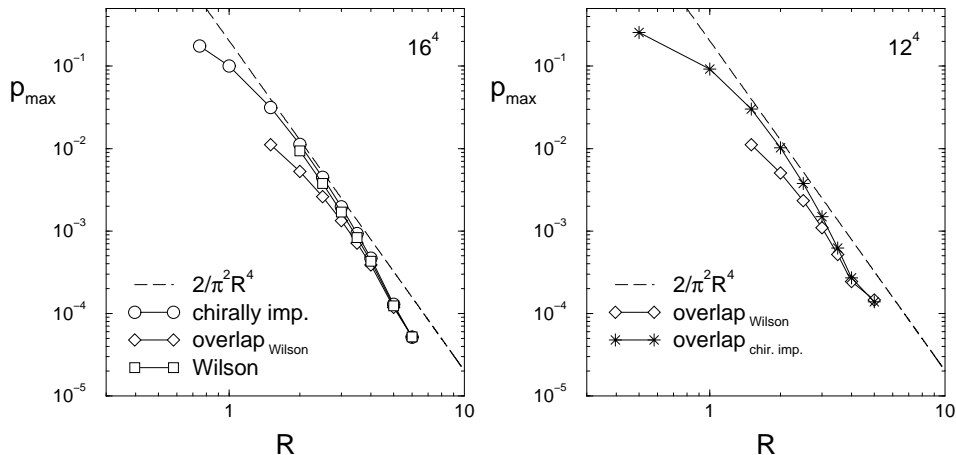


Figure 4: The maximum  $p_{max}$  of  $p(x)$  as a function of the radius  $R$  of the underlying instanton. In the plot on the left-hand side we show our results on  $16^4$  lattices for the Wilson overlap operator (diamonds), the chirally improved operator (circles) and the Wilson operator (squares). The right-hand side plot provides a comparison of the Wilson overlap operator and the chirally improved overlap operator on  $12^4$  lattices.

the Wilson operator also follows the continuum curve quite well.

The situation is different for the Wilson overlap operator. Already at  $R = 3.5$  the zero mode of the Wilson overlap operator has a value of the inverse participation ratio which is visibly different from the continuum result, and the error quickly increases as  $R$  is decreased (note the logarithmic scale). At  $R = 2.5$  the Wilson overlap result amounts to only 60% of the continuum formula and at  $R = 1.5$  only about 30% remain.

In the plot on the right-hand side of Fig. 3 we compare the inverse participation ratio of the Wilson overlap operator (diamonds) to the inverse participation ratio of the zero mode of the chirally improved overlap operator (asterisks). It is obvious that with the chirally improved overlap operator the results for small instantons are considerably closer to the continuum line.

A second characteristic quantity of the zero mode is the maximum  $p_{max}$  of  $p(x)$ , which in the continuum is given by  $p_{max} = p(0) = 2/(\pi^2 R^4)$ . In Fig. 4 we plot our data for this quantity as a function of the instanton radius  $R$ .

Again the left-hand side plot shows the results for the chirally improved operator, the Wilson operator and the Wilson overlap operator, while the right-hand side compares the Wilson overlap operator with the chirally improved overlap operator. The overall picture is similar to the results for the inverse participation ratio. The chirally improved operator gives the best results, while the Wilson overlap operator has again problems with reproducing the continuum results for smaller instantons. One finds that the amount of the deviation of the Wilson overlap result from the continuum formula is already 50% at  $R = 2.5$  and increases further for smaller  $R$ . The situation is improved when using the chirally improved overlap operator.

We remark that we performed the same analysis with two changes of our setting: (1) Instead of using 1 as the center for the overlap projection we also used  $1 + s$ , with  $s = 0.1$ ,  $s = 0.2$  and  $s = 0.5$ . Such an adjustment of the center of the projection is known [17] to optimize the localization properties of the Wilson overlap operator. We found that a variation of  $s$  amounts to only small changes of  $I$  and  $p_{max}$  for the zero modes of the Wilson overlap operator. (2) We also used a different discretization of the continuum instanton. We placed the instanton at the center of a hypercube. This allowed us to shrink the “inner part” of the gauge potential such that it only consisted of the interior of this hypercube, and we could then use the potential in the singular gauge on the whole lattice. Also this modification does not change the picture we obtained and shows that the results are not very sensitive to the details of the discretization of the instanton.

To summarize, we find that the Wilson overlap operator has significant problems with reproducing the continuum zero mode for instantons with  $R \leq 2.5$ , while the other operators, i.e. the chirally improved operator, the Wilson Dirac operator and the chirally improved overlap operator do not show such a large deviation from the continuum result.

Why does the chirally improved overlap operator reproduce the continuum results better than the Wilson overlap Dirac operator? Possibly this is connected with the fact that the input Dirac operator in the chirally improved case is already a much better approximation to a Ginsparg-Wilson operator than the Wilson operator.

For a typical simulation with  $a \sim 0.1$  fm, our results for the Wilson overlap operator imply that structures smaller than  $\sim 0.3$  fm will probably not be resolved properly. We expect that the chirally improved operator with or without additional overlap projection fares better for such small structures.

**Acknowledgements:** We would like to thank Tom DeGrand, Peter Hasenfratz, Ivan Hip and Karl Jansen for interesting discussions. This

project was supported by the Austrian Academy of Sciences, the DFG and the BMBF. We thank the Leibniz Rechenzentrum in Munich for computer time on the Hitachi SR8000 and their operating team for training and support.

## References

- [1] P.H. Ginsparg and K.G. Wilson, Phys. Rev. D 25 (1982) 2649.
- [2] R. Narayanan and H. Neuberger, Phys. Lett. B 302 (1993) 62, Nucl. Phys. B 443 (1995) 305.
- [3] P. Hasenfratz, Nucl. Phys. B (Proc. Suppl.) 63 (1998) 53; P. Hasenfratz, Nucl. Phys. B 525 (1998) 401; P. Hasenfratz, V. Laliena and F. Niedermayer, Phys. Lett. B 427 (1998) 353; P. Hasenfratz, S. Hauswirth, K. Holland, Th. Jörg, F. Niedermayer and U. Wenger, Int. J. Mod. Phys. C 12 (2001) 691.
- [4] P.M. Vranas, Nucl. Phys. Proc. Suppl. 94 (2001) 177.
- [5] C. Gattringer, Phys. Rev. D 63 (2001) 114501; C. Gattringer and I. Hip, Phys. Lett. B 480 (2000) 112.
- [6] C. Gattringer, I. Hip and C.B. Lang, Nucl. Phys. B597 (2001) 451.
- [7] T. De Grand and A. Hasenfratz, hep-lat/0103002.
- [8] R.G. Edwards and U.M. Heller, hep-lat/0105004.
- [9] C. Gattringer, M. Göckeler, P.E.L. Rakow, S. Schaefer and A. Schäfer, hep-lat/0105023 (Nucl. Phys. B in print) and hep-lat/0107016 (Nucl. Phys. B in print).
- [10] T. Blum, N. Christ, C. Cristian, C. Dawson, X.Liao, G. Liu, R. Mawhinney, L. Wu and Y. Zhestkov, hep-lat/0105006.
- [11] I. Horváth, N. Isgur, J. McCune and H. B. Thacker, hep-lat/0102003.
- [12] T. Schäfer and E.V. Shuryak, Rev. Mod. Phys. 70 (1998) 323; D. Diakonov, Talk given at International School of Physics, 'Enrico Fermi', Course 80: Selected Topics in Nonperturbative QCD, Varenna, Italy, 1995, hep-ph/9602375.

- [13] T. Banks and A. Casher, Nucl. Phys. B169 (1980) 103.
- [14] I. Hip, Th. Lippert, H. Neff, K. Schilling and W. Schroers, hep-lat/0105001.
- [15] T. DeGrand and A. Hasenfratz, Phys. Rev. D 64 (2001) 034512.
- [16] W. Bietenholz, Eur. Phys. J. C 6 (1999) 537.
- [17] P. Hernandez, K. Jansen and M. Lüscher, Nucl. Phys. B 552 (1999) 363.
- [18] P. Hernandez, K. Jansen and L. Lellouch, *A numerical treatment of Neuberger's lattice Dirac operator*, in: Lecture Notes in Computational Science and Engineering 15, A. Frommer, T. Lippert, B. Medeke, K. Schilling (Eds.), Springer, Berlin 2000.
- [19] I.A. Fox, M.L. Laursen, G. Schierholz, J.P. Gilchrist and M. Göckeler, Phys. Lett. B158 (1985) 332.
- [20] D.C. Sorensen, SIAM J. Matrix Anal. Appl. 13 (1992) 357; R. B. Lehoucq, D.C. Sorensen and C. Yang, ARPACK User's Guide, SIAM, New York, 1998.
- [21] I. Horváth, Phys. Rev. Lett. 81 (1998) 4063, Phys. Rev. D 60 (1999) 034510; W. Bietenholz, hep-lat/9901005.
- [22] S. Itoh, Y. Iwasaki and T. Yoshié, Phys. Rev. D36 (1987) 527, Phys. Lett. B 184 (1987) 375.